

This is the accepted manuscript made available via CHORUS. The article has been published as:

Screw-dislocation constrictions in face-centered cubic crystals

Enrique Martínez and John P. Hirth

Phys. Rev. B **90**, 064102 — Published 4 August 2014

DOI: [10.1103/PhysRevB.90.064102](https://doi.org/10.1103/PhysRevB.90.064102)

Screw Dislocation Constrictions in Face-Centered Cubic Crystals

Enrique Martínez^{1,*} and John P. Hirth²

¹*Material Science and Technology Division, MST-8,
Los Alamos National Laboratory, Los Alamos, 87545 NM, USA*

²*Center for Integrated Nanotechnology, Los Alamos National Laboratory, Los Alamos, 87545 NM, USA*
(Dated: July 17, 2014)

We show, using molecular statics and dynamics simulations along with dislocation dynamics calculations, that the structure of a screw dislocation in a thin film or at a free surface for face-centered cubic Cu differs from that found in bulk. In agreement with earlier work, a screw dislocation at the surface is observed to dissociate in two different $\{111\}$ planes, forming a constriction at the site where the glide plane changes. We analyze in detail the energetics of the structure and conclude that the constricted configuration is stable due to the long-range elastic interactions. We have also performed shear stress simulations and compared to bulk stress to understand how the constriction modifies the response of the dislocation to an applied load. We found that such constriction represents a strong pinning point, substantially increasing the yield stress required for the dislocation to glide. In contrast, the configuration provides a barrierless source for the dislocation to cross slip.

PACS numbers:

Keywords: **Dislocations, Thin Films, Mechanical Response**

I. INTRODUCTION

Modeling and simulation provide valuable insight in the structure and deformation process in thin films and nanomaterials¹⁻³. Molecular dynamics (MD) calculations⁴ have been performed to study the growth of Cu thin films on different substrates^{5,6} and the stress response and dislocation nucleation in pristine films⁷⁻⁹. The dislocation dynamics (DD) methodology has been applied to study the mechanical properties of thin films¹ (and references therein) as well as junction formation and jogs in free-standing face-centered cubic (fcc) films^{10,11}. In earlier MD and DD simulations¹² we observed stable constrictions at a site where a screw dislocation dissociates onto two different $\{111\}$ planes in small angle $\{100\}$ twist boundaries in Cu. The reason for this configuration to appear was not clear because of the complicated structures forming at the dislocations nodes, where the constrictions originated. It was suggested¹³ that such constrictions might be stable in thin films. The basic reason for this is the self-torque that tends to rotate a dislocation line segment into the low line energy screw configuration¹⁴ and such rotations can be readily achieved at free surfaces. Rasmussen *et al.*¹⁵ used the self-torque concept to explain the activation energy for a screw dislocation to cross-slip in Cu by the Friedel-Escaig mechanism^{16,17}, using an effective medium theory. The authors studied the case of screw dislocation lines normal to a free surface, making the important contribution that the two constrictions needed for this process to occur are not equivalent. In one case, the dislocation segments around the constriction are screw in character while on the other, the dislocations are mostly edge in character. The line energy of the former is low and the latter high. We follow their terminology and call the paired segments adjoining the constriction screw-like and edge-like. They calculated the energy of both constrictions, with the in-

teresting result that the energy of a dislocation containing a screw-like constriction is lower than that of a simple dissociated straight dislocation. They did not determine the reason for this but imply that it is not a linear elastic effect. The authors also studied the effect of free surfaces on the dislocation configuration and concluded that the orientation of the surface steps determines the stability of the constriction. Christiansen *et al.*¹⁸ combined experiments with modeling in Ag to study the dislocation structure at free surfaces. Using MD, the authors found the configuration with one open end and a constricted end extended in a unique $\{111\}$ plane to be the most stable configuration while the experiments did not reveal any constricted end at the surface.

More recently, Rao *et al.*²⁰ have performed atomistic simulations of this surface cross-slip process in Cu and Ni. For both the cases of dislocations inclined to a $\{100\}$ surface and perpendicular to a $\{110\}$ surface, they found that the self-torque did not always overcome image effects so that constrictions did not always form. A value of -1.3 eV for the screw-like constriction was inferred from those calculations, which, as we shall see, is in close agreement with our results. Nudged-Elastic band calculations were also performed to obtain the activation barrier for cross-slip near the surface with a value for Cu of 0.09 eV.

In the present article we use DD calculations, molecular statics (MS) and MD together with theoretical analysis to study a screw dislocation in a thin film of Cu and other fcc metals. We show that the constriction is indeed energetically favorable with respect to the dislocation dissociated on one plane in fcc free-standing Cu thin films, in agreement with Refs. 15,18-20. We also find that there is a weak repulsive force acting to move a constriction away from the free surface. This force is associated with a long-range elastic interaction between segments adjacent to a constriction, and effect additional to the torque

TABLE I: Energy values as given by DD calculations for the configurations [b], [c] and [d] relative to [a] in Fig. 1.

STRUCTURE	EDGE-LIKE [b]	SCREW-LIKE [c]	COPLANAR [d]
ΔW_E (eV)	13.47	-5.16	4.10
ΔW_F (eV)	-0.38	-0.97	-0.46
ΔW_T (eV)	13.09	-6.13	3.64

and image terms considered previously^{15,18–20}. We study the mechanical response of the system to simple shear loading and observe that the constriction substantially modifies the dislocation mobility, acting as a strong pinning point.

II. RESULTS AND DISCUSSION

A. Dislocation dynamics calculations of constriction energies

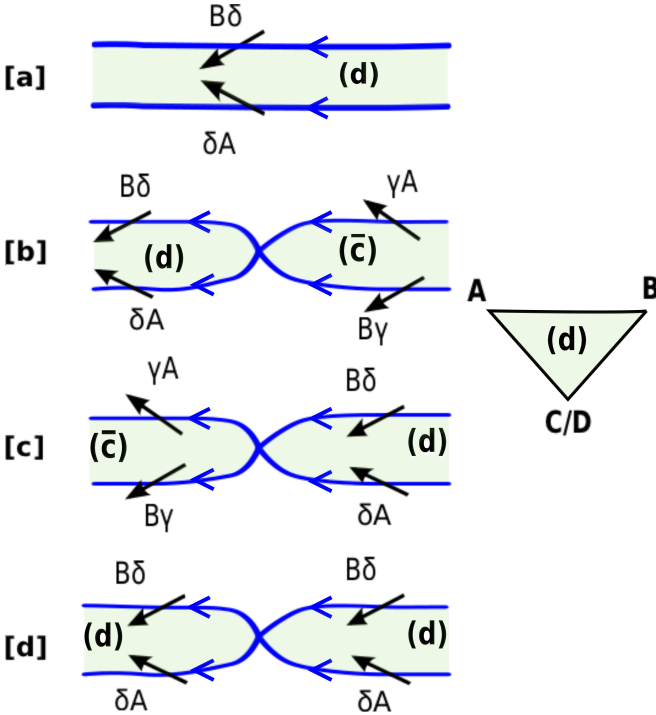


FIG. 1: Sketches with three possible configurations that the screw dislocation might adopt in free-standing fcc thin films: [a] Parallel Shockley partials; [b] Edge-like constriction; [c] Screw-like constriction; and [d] Coplanar constriction.

In bulk Cu, screw dislocations dissociate into Shockley partials in a $\{111\}$ plane, with no indication from

TEM observations or simulations that any constrictions tend to be present. We tested this observation in DD by comparing the energy of the dissociated dislocation with three different types of constriction as indicated in Fig. 1. In the usual way, the dislocations are approximated by straight-line segments, and their self and interaction energies are summed. For the DD calculations isotropic elasticity is assumed. The core energy is empirically represented by a linear core cutoff for adjacent segments as in the Paradise code²¹. The interfacial free energy of the intrinsic faults is also included²². The energies are listed in Table I relative to the energy of two parallel partials on one plane. The relative total energy W_T , elastic energy W_E and stacking fault energy W_F are shown. The fault term is small compared to the elastic energy. Relatively, $W_c < W_a < W_d < W_b$. Configuration [b] has all edge-like segments and [d] has two edge-like segments and two screw-like segments. The high energy of the edge-like segments accounts for the relatively high energies of these configurations. Configuration [c] has all screw-like segments. In agreement with Rasmussen *et al.*¹⁵, it has a lower energy than the straight dislocation [a]. Two factors can contribute to this unusual result. First, the screw-like segments have lower self energies than the mixed partials in [a]. Second, the long segments on different glide planes have a lower long-range interaction energy with one another than the coplanar segments. The latter interaction is given explicitly in the DD calculations but would be difficult to isolate in MD or MS computations. This difference appears later as well. Essentially, the energy of a screw dislocation is lowered by dissociation into as many partial or fractional dislocations as possible. Thus, in bcc crystals there is a tendency for screw dislocations to dissociate into fractional dislocations on 3 or 6 planes, despite associated large fault energy²³. For a cylindrical precipitate formed on a screw dislocation, the dislocation dissociates into a continuous distribution of infinitesimal dislocations on the surface of the precipitate²⁴, with an even larger relative decrease in energy.

We now consider the thin film case. The presence of the surfaces introduces degrees of freedom that allow the dislocation to modify its structure to lower the system energy. In this scenario, three configurations would be possible: (i) a constriction is formed and two open ends appear; (ii) no constriction develops and an open end and a closed end form with the dislocation split in a unique $\{111\}$ plane; and (iii) a constriction forms and two closed ends develop. Figure 2 shows schematics of these three possible configurations. We again use DD to calculate the energies of these configurations. Added image interactions are included to comply with the free surface boundary condition.

The energies are given in Table II with respect to the parallel Shockley partials configuration. The energy sequence in this case is $W_a < W_b < W_c$. Configuration [a] has a screw-like constriction and screw like ends, as well as non-coplanar long segments as in the previous anal-

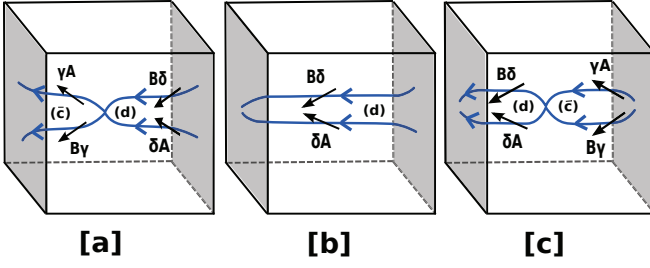


FIG. 2: Sketches with three possible configurations that the screw dislocation might adopt in free-standing fcc thin films: [a] Two open ends plus one screw-like constriction; [b] One open end and one closed end; and [c] Two closed ends plus one edge-like constriction.

TABLE II: Energy values as given by DD calculations for the configurations [a], [b] and [c] in Fig. 2 relative to the parallel Shockley partials configuration.

STRUCTURE	[a]	[b]	[c]
ΔW_E (eV)	-17.27	-9.95	6.65
ΔW_F (eV)	\sim	\sim	-0.74
ΔW_T (eV)	-17.27	-9.95	5.91

ysis of Fig. 1. Both effects favor the lowest energy for configuration [a]. The pair of edge-like segments disfavor configuration [c]. In Fig. 1, configurations [a] and [b] show two screw-like ends, so the same factors favoring [b] in Fig. 1 apply for [a] in Fig. 2. Moreover, in an anisotropic material like Cu, the ratio between energy coefficients is given by $K_s/K_e = 0.56$, with $K_s = 42.2$ GPa and $K_e = 75.5$ GPa, which is lower than for the isotropic case where $K_s^i/K_e^i = (1 - \nu) = 0.68$ (ν is the Poisson coefficient)¹⁴. This shows that in the anisotropic elastic case, the torque favoring screw-like segment character is greater than in the isotropic case. This further strengthens the trends presented in Tables I and II.

B. Molecular static calculations of constriction stability

One key element that is missing in the DD calculations is the core-core dislocation interaction. This element, along with the anisotropy, is naturally included in MS/MD models, and therefore, we use this later methodology to assess the role of these two contributions in the formation of the constriction.

We generated a screw dislocation in Cu using linear elasticity¹⁴. The computational volume is oriented in the $[\bar{1}\bar{1}2]$, $[1\bar{1}0]$ and $[111]$ directions with total dimensions $26.5 \times 43 \times 44$ nm³, containing 4.032 million atoms and the dislocation line lying along the $[1\bar{1}0]$ direction

with a Burgers vector of $\frac{1}{2}[1\bar{1}0]$ with the dislocation line midway between the (111) surfaces. Image forces are negligible at the center of the 44 nm sample height so free (111) surfaces suffice to simulate bulk behavior, and therefore free boundary conditions were applied in the $[111]$ direction. In the bulk calculations periodic boundary conditions were applied in the other two directions while in the case of the thin film free surfaces were created normal to the direction of the dislocation line (threading dislocation) and periodic in the remaining direction (see Fig. 3).

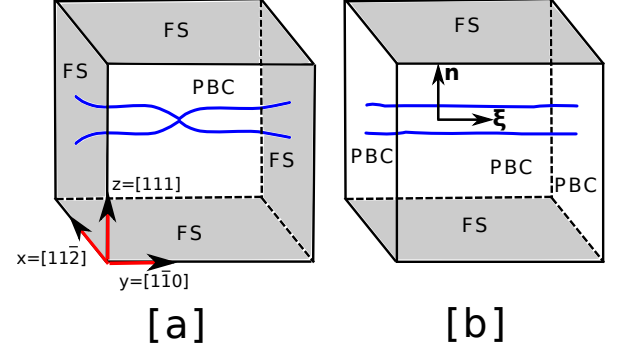


FIG. 3: MS and MD simulation boundary conditions. [a] Boundary conditions used to study the constriction formation with four free surfaces (FS) in the y and z directions and periodic boundary conditions (PBC) in the x direction and; [b] boundary conditions utilized to calculate bulk properties, with FS in the z direction and PBC in x and y.

This method automatically includes the surface step associated with the emerging screw segment. The LAMMPS code²⁶ with the Mishin *et al.* interatomic potential²⁷ was used to perform the simulations. We did not examine the nucleation process, but the appearance of the constriction is consistent with the low nucleation energies calculated in Ref. 20. After minimizing the sample using a conjugate gradient algorithm we observe the formation of a constriction close to the mid-point between surfaces. We have tested the stability of this configuration by running MD for 1 ns at 300 K in the NPT ensemble with a time step of 1 fs. During the dynamic run the constriction moves in an oscillatory way along the dislocation line, even reaching the surface at various occasions and reforming thereafter. Following the dynamics, a conjugate gradient algorithm was performed to reach a minimum energy configuration, which was observed to contain the screw-like constriction near the center of the film (see Fig. 4), agreeing with Fig. 2[a].

If we assume that the surface energy is the same in all possible configurations and we consider a semi-infinite approximation (*i.e.* the interaction between the dislocation segments near the surface and the mid constriction is considered negligible), the energies with respect to the straight dissociated dislocation (Fig. 5[a]) of the configurations shown in Fig. 2 can be subdivided into four

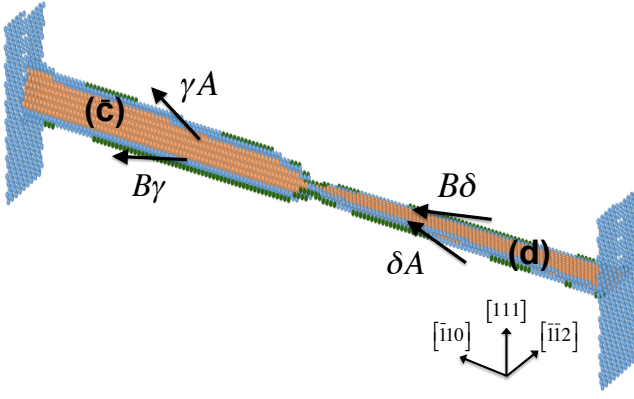


FIG. 4: Screw dislocation configuration in free-standing Cu thin films. Atoms are colored according to a common neighbor analysis²⁸, with hcp atoms in orange, bcc atoms in green and atoms in nonlinearly perturbed positions in blue.

different components: open end, screw-like constriction, edge-like constriction and closed end. From the DD results we know that the configuration [c] in Fig. 5 would be energetically unfavorable. The energy with respect to the straight dislocation (Fig. 5[a]) for each configuration can then be written as

$$\begin{aligned} W[a] &= 2 \cdot W^{OP} + W^{CS} \\ W[b] &= W^{OP} + W^{CL} \\ W[c] &= 2 \cdot W^{CL} + W_*^{CS} \end{aligned} \quad (1)$$

where W^{OP} is the energy of the open configuration, W^{CS} is the energy of the screw-like constriction, W^{CL} is the energy of the closed arrangement and W_*^{CS} is the energy of the edge-like constriction.

To calculate the energy of the straight dislocation configuration we have relaxed a screw dislocation with periodic boundary conditions along the dislocation line, whereupon the dislocation dissociates on one $\{111\}$ plane. We then introduce surfaces at both ends of the dislocation line, fix the positions of the atoms with a distance larger than 1 nm from the surface and subsequently minimize further the energy of the structure (Fig. 5[a]). This setup ensures that the atoms at the surface are initially relaxed, since it has been shown that relaxations normal to the surface are confined to about 1 nm³⁷. To construct a single closed configuration, the sample with the straight dislocation was further relaxed with a fixed layer of atoms in a region from the middle of the sample to 1 nm from the surface to ensure that the semi-infinite approximation holds (Fig. 5[b]). We have repeated the same approach to calculate the energy of a single open configuration, fixing the atomic positions at the opposite dislocation end (Fig. 5[c]). When every atom is free to move, the relaxed configuration shows the formation of the constriction near the mid-point of the dislocation line (Fig. 5[d]). Table III shows the values of the en-

TABLE III: Energy values as given by MS calculations for the open, closed and constriction configurations as shown in Figures 5[b], 5[c] and 5[d].

STRUCTURE	CLOSED	OPEN	CONSTRICTION
ΔW (eV)	-180.98	-184.54	-370.71

ergy relative to that of Fig. 5[a] for these three different configurations, *i.e.* open, closed and the one with the constriction.

Using the above values in Eq. 1 we estimate the value of the screw-like constriction of Fig. 2[a] to be $W^{CS} \approx -1.64$ eV. The value is in good agreement with the one obtained by Rasmussen *et al.*¹⁵ and by Rao *et al.*²⁰. Although small, the negative sign is interesting: together with the small nucleation energies computed in Ref. 20, the result implies easy formation of the constriction provided that the dislocation is subject to the right constraints. The fact that no closed constriction is observed experimentally at the surface¹⁸ is consistent with the results presented in this study. The energy of configuration [b] in Fig. 2 becomes $W[b] = -365.51$ eV, in agreement with the MS results where the structure relaxes directly to the open configuration ($W[a] = -370.71$ eV). Thus the MS results agree with the DD results: the configuration with screw-like segments and ends has lower energy than a straight dislocation dissociated on one plane. Yet the effect is less marked in the MS case, suggesting a role of core interactions. The results also imply that for thick crystals at a free surface, a constriction should be stable in the near-surface region. However, the end effects are important, and the energy of a screw-like constriction is only slightly less than a straight coplanar configuration as shown by the present MS results as well as earlier studies^{15,20}. The DD calculations indicate a larger stability for a constriction, but the DD results perform neglect core repulsions. The absolute energy values of the energy differences in the DD and MS calculations differ in part because of different reference states. The near surface configuration in Fig. 5[a] has a much higher energy than that in Fig. 1[a]. In addition, core repulsion and elastic anisotropy are included in the MS calculations but not the DD results. The finding that the equilibrium position for the constriction is in the middle of the thin film, with scatter about that position, indicates that the constrictions are weakly repelled from the surface. Near the surface the long-range image interaction performs with coplanar image dislocations, resembling Fig. 1[d]. In contrast, away from the surface, the long-range interactions are non-coplanar as in Fig. 1[c]. As discussed previously, the latter repulsive forces are greater than the former, giving a lower constriction energy.

Nonlinear core configurations can be represented by sets of line force dipoles or dislocation dipoles^{29,30}. These

are of the same sign for a given type of dislocation and therefore would qualitatively predict core-core repulsion. On the other hand overlapping cores limit the core volume and could represent a short-range attraction. The core field exerts an additional force on the dislocations that is proportional to the gradient of the core stress field. The MS results imply that the former effect is more important. Second-order image effects could also have a role in the MS results.

While step energy would contribute to loop nucleation at the surface, it has a second-order effect here and did not influence the configurations at the surface significantly, in disagreement with an earlier postulate¹⁵. The reason is that the step line tension on the dislocation acts in the same direction with one half of the net force acting on each partial. Hence the step could in principle bend both partials in the same direction but would not affect the net opening at the ends to first order.

We briefly addressed size effects. The constriction formed for all dislocation line lengths in Cu, *i.e.*, any distance between surfaces, even as low as 2.2 nm. Moreover, we have tested the existence of the constriction in different fcc elements (Ni³³, Al³⁴, Au³⁵ and Ag³⁶) and it was observed in all of them. In this sense, the different geometries in Refs. 12,15,18 and the present work, compared to Rao *et al.*²⁰ inclined configuration is of interest. The configuration of a screw normal to the surface in the former set maximizes the long-range (actual or image) segment interactions and minimizes the initial image force resisting curvature associated with the self-torque term. The latter configuration²⁰, entails a large angle between the screw sense vector ξ and the surface normal \mathbf{n} . In comparison to the former case, this lessens the long-range segment interaction and increases the image interaction resisting the self-torque term. These differences could produce a change in nucleation behavior. The work in Ref. 20 is symmetric in the sense that $\xi \times \mathbf{n}$ is a vector that lies in the plane of the surface. For lower symmetry other effects could appear such as local bending of the entire dislocation near the surface. In addition, if local climb can occur, jog formation, which would provide added pinning, could occur near the surface for all cases where ξ is not parallel to \mathbf{n} .

C. Response to shear loading

We have also studied the system response to an external simple shear applied on the $\{111\}$ glide plane. The stress was applied along the Burgers vector direction, at a strain rate of 10^9 s^{-1} and a temperature of 300 K. Figure 6[a] shows the stress-strain curve for both the thin film and bulk systems. In bulk, in the absence of strong pinning points, screw dislocations in Cu move freely under phonon damping control since their Peierls barrier is small²². However, the presence of the constriction modifies this picture significantly. While the constriction exists the stress increases linearly with strain. For the dis-

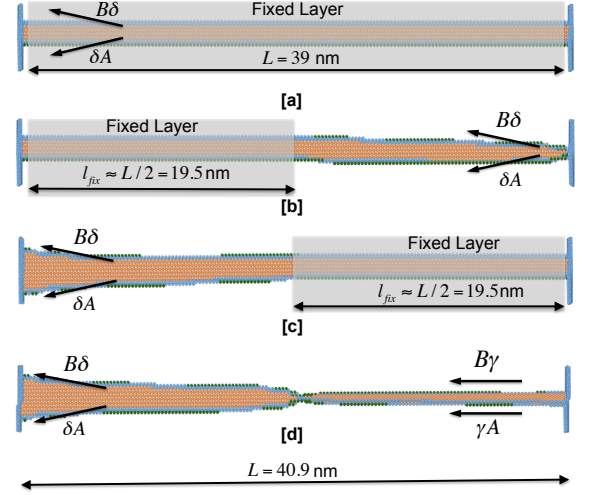


FIG. 5: Four different screw dislocation configurations in a Cu thin film: [a] Straight dislocations; [b] closed configuration; [c] open structure; and [d] dislocation dissociated in two different $\{111\}$ plane with a constriction formed near the mid point between surfaces.

location to move the constriction has to be annihilated at one surface. Shaded areas in Fig. 6[a] indicate regions where the constriction has been removed and the dislocation is free to move. Those regions coincide with a sudden release of stress. Figure 6[b] shows a series of snapshots of the process. At (1) the constriction has just been annihilated and the dislocation starts to glide. The stress drops significantly until the constriction is re-formed at time (2) and the stress starts to build up further. At (3) the constriction is annihilated again, with the dislocation gliding in the cross-slip plane. At that point there is an abrupt decrease in stress and the dislocation glides freely for the rest of the calculation (4). These results show that the constriction acts as a strong pinning point for the dislocation moving on the primary glide plane, producing substantial hardening. With more convoluted loadings favoring slip on the cross slip plane the response would be more complex.

We emphasize, in agreement with Rao *et al.*²⁰, that the stress response presented in Fig. 6 applies for a single dislocation (as in Fig. 5) and that only one constriction ever forms. Added constrictions could only form in screw-like and edge-like pairs as discussed by Rasmussen *et al.*¹⁵. Thus, for extensive cross-slip, the single cross-slip dislocation would have to interact to form a continuing source, *e.g.*, as a spiral source. These pairs have a large, positive, formation energy and would only occur at large driving forces.

There are additional phenomena associated with the constriction. The first relates to internal friction. The motion of the constriction along the dislocation line provides an internal friction mechanism that dissipates en-

ergy. This mechanism should be particularly effective in damping surface Rayleigh waves³¹ and interface Stonely waves³². The second relates to cross slip. As already shown¹⁵, there should be a negligible activation energy for cross slip of a screw in the near surface region. A portion of the line already lies on the cross slip plane and it can move readily under stress states favoring cross slip.

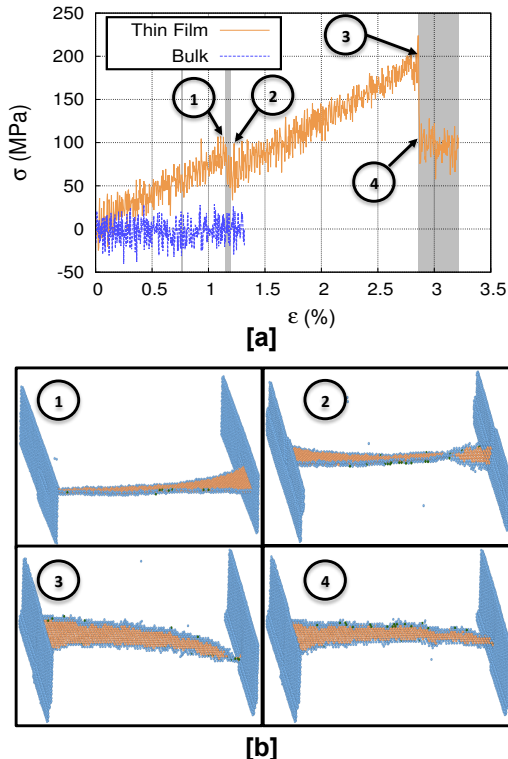


FIG. 6: [a] Stress-strain curve for a threading screw dislocation with a constriction formed. Shaded areas represent region where the constriction was annihilated. The numbers match the snapshots with the dislocation configuration along the deformation process shown in figure [b]. Atoms are colored according to a common neighbor analysis²⁸, with hcp atoms in orange, bcc atoms in green and atoms in nonlinearly perturbed positions in blue.

III. CONCLUSIONS

In summary, we report on DD and MS/MD results of a screw dislocation configuration in fcc free-standing Cu

thin films. The dislocation splits into Shockley partials in two different $\{111\}$ planes, forming a screw-like constriction near the middle point between surfaces. We have analyzed in detail the energetics of the configuration obtaining an estimate for the constriction energy, as well as for the open and closed surface configurations relative to the straight dislocation. DD provides a good estimate of the relative energies between different configurations (Tables I and II) and isolates the long-range segment interactions, but perforce does not include anisotropic factors and the core-core interactions that are included in MS. The MS results show that the energy of the screw-like constriction is slightly negative, with a calculated value of $W^{CS} \approx -1.64$ eV, in agreement with previous works^{15,19,20}, and the configuration with two open ends plus the constriction is the most energetically favorable. These results are consistent with the observation that no closed end is found experimentally¹⁸ at the surface of an fcc Ag crystal. Novel observations in the present work include: (i) the surface structure has no first-order effect on the results; (ii) the repulsive long-range interaction energy between parallel segments has a significant effect and; (iii) the stable position for the constriction in a thin film is at the film center. The earlier results^{15,18–20} were extended to show that the constrictions are stable in a number of fcc metals and that the stability in a thin film is independent of film thickness. We have also studied the mechanical response of the system to simple shear loading. We observe that the stress required for the dislocation to move is much higher than for a dislocation gliding in bulk. The dislocation glides in a discontinuous fashion, accumulating strain energy when the constriction is formed and moving rapidly under damping control when the constriction is annihilated. We conclude that the screw-like constriction provides a strong pinning point and is a factor influencing constitutive representations of deformation behavior.

IV. ACKNOWLEDGMENTS

The authors gratefully acknowledge the support from the Center for Materials at Irradiation and Mechanical Extremes, an Energy Frontier Research Center funded by the U.S. Department of Energy (Award Number 2008LANL1026) at Los Alamos National Laboratory, as well as helpful discussions with A. Caro. Parallel computations were performed on the Lobo machine at the High Performance Computing clusters at Los Alamos National Laboratory.

* Electronic address: enrique.m@lanl.gov

¹ O. Kraft, P. A. Gruber, R. Mönig, D. Weygand, *Ann. Rev. Mater. Res.* 40 (2010) 293–317.

² J. R. Greer, J. T. M. D. Hosson, *Prog. in Mat. Sci.* 56

(2011) 654–724.

³ A. Misra, J. P. Hirth, R. G. Hoagland, *Acta Mater.* 53 (2005) 4817–4824.

⁴ D. Frenkel, B. Smit, *Understanding Molecular Simulation*,

- Academic Press, 2001.
- ⁵ J. Zhang, C. Liu, Y. Shu, J. Fan, AIP Conf. Proc. 1501 (2012) 919.
 - ⁶ T. P. C. Klaver, B. J. Thijssse, J. Comp.-Aided Mat. Des. 10 (2003) 61–74.
 - ⁷ Y. Umeno, T. Shimada, T. Kitamura, Phys. Rev. B 82 (2010) 104108.
 - ⁸ A. V. Bolesta, V. M. Fomin, Physical Mesomechanics 12 (2009) 117–123.
 - ⁹ A. V. Bolesta, V. M. Fomin, Physical Mesomechanics 14 (2011) 107–111.
 - ¹⁰ C. R. Weinberger, S. Aubry, S.-W. Lee, W. D. Nix, W. Cai, Modelling Simul. Mater. Sci. Eng. 17 (2009) 075007.
 - ¹¹ S.-W. Lee, S. Aubry, W. D. Nix, W. Cai, Modelling Simul. Mater. Sci. Eng. 19 (2011) 025002.
 - ¹² E. Martinez, J. P. Hirth, M. Nastasi, A. Caro, Phys. Rev. B 85 (2012) 060101(R).
 - ¹³ J. P. Hirth, J. Supercond Nov Magn 25 (2012) 561–563.
 - ¹⁴ J. P. Hirth, J. Lothe, Theory of Dislocations, 2nd Edition, Krieger, 1982.
 - ¹⁵ T. Rasmussen, K. W. Jacobsen, T. Leffers, O. B. Pedersen, Phys. Rev. B 56 (6) (1997) 2977–2990.
 - ¹⁶ J. Friedel, Dislocations and Mechanical Properties of Crystals, Wiley, 1957.
 - ¹⁷ B. Escaig, Journal de Physique 29 (1968) 225.
 - ¹⁸ J. Christiansen, K. Morgenstern, J. Schiøtz, K. Jacobsen, K.-F. Braun, K.-H. Rieder, E. Lægsgaard, F. Besenbacher, Phys. Rev. Lett. 88 (20) (2002) 206106.
 - ¹⁹ S. I. Rao, T. A. Parthasarathy, C. Woodward, Phil. Mag. 79 (1999) 1167–1192.
 - ²⁰ S. I. Rao, D. M. Dimiduk, T. A. Parthasarathy, M. D. Uchic, C. Woodward, Acta Mat. 61 (2013) 2500–2508.
 - ²¹ A. Arsenlis, W. Cai, M. Tang, M. Rhee, T. Oppelstrup, G. Hommes, T. G. Pierce, V. V. Bulatov, Modelling Simul. Mater. Sci. Eng. 15 (2007) 553–595.
 - ²² E. Martinez, J. Marian, A. Arsenlis, M. Victoria, J. M. Perlado, Journal of the Mechanics and Physics of Solids 56 (2008) 869–895.
 - ²³ L.H. Yang, M. Tang and J.A. Moriarty, Dislocations in Solids, vol. 16, eds. J.P. Hirth and L. Kubin, Elsevier, Amsterdam, 2010, p. 1
 - ²⁴ R. Gomez-Ramirez, G. M. Pound, Metall. Trans. 4 (1973) 1563.
 - ²⁵ W. Cai, Md++.
URL <http://micro.stanford.edu/MDpp/docs>
 - ²⁶ S. Plimpton, Journal of Computational Physics 117 (1995) 1–19.
 - ²⁷ Y. Mishin, M. J. Mehl, D. A. Papaconstantopoulos, A. F. Voter, Phys. Rev. B 63 (2001) 224106.
 - ²⁸ A. Stukowski, Modelling Simul. Mater. Sci. Eng. 18 (2010) 015012.
 - ²⁹ P. C. Gehlen, J. P. Hirth, R. G. Hoagland, M. F. Kanninen, J. Appl. Phys. 43 (1972) 3921–3933.
 - ³⁰ E. Clouet, Phys. Rev. B 84 (2011) 224111.
 - ³¹ J. Lothe, Amsterdam, 1992, p. 447.
 - ³² D. M. Barnett, J. Lothe, S. D. Gavazzaz, M. J. P. Musgrave, Proc. Roy. Soc 402A (1985) 153.
 - ³³ A. F. Voter, A. P. Chen, Mater. Res. Soc. Symp. Proc. 82 (1987) 175.
 - ³⁴ X. Liu, F. Ercolessi, J. B. Adams, Modelling Simul. Mater. Sci. Eng. 12 (2004) 665–670.
 - ³⁵ G. J. Ackland, G. I. Tichy, V. Vitek, M. W. Finnis, Phil. Mag. A 56 (1987) 735–756.
 - ³⁶ P. L. Williams, Y. Mishin, J. C. Hamilton, Modelling Simul. Mater. Sci. Eng. 14 (2006) 817.
 - ³⁷ S. P. Chen, A. F. Voter and D. J. Srolovitz, Phys. Rev. Lett. 57 (1986) 1308